

See discussions, stats, and author profiles for this publication at: <https://www.researchgate.net/publication/23999754>

A potential of mean force estimator based on nonequilibrium work exponential averages

ARTICLE *in* PHYSICAL CHEMISTRY CHEMICAL PHYSICS · MARCH 2009

Impact Factor: 4.49 · DOI: 10.1039/b810914c · Source: PubMed

CITATIONS

19

READS

14

2 AUTHORS:



Riccardo Chelli

University of Florence

89 PUBLICATIONS 1,781 CITATIONS

SEE PROFILE



Piero Procacci

University of Florence

117 PUBLICATIONS 2,104 CITATIONS

SEE PROFILE

A potential of mean force estimator based on nonequilibrium work exponential averages

Riccardo Chelli^{*ab} and Piero Procacci^{ab}

Received 26th June 2008, Accepted 6th November 2008

First published as an Advance Article on the web 8th January 2009

DOI: 10.1039/b810914c

In this article we present a potential of mean force estimator based on measurements of the work performed on a system during out of equilibrium realizations of a process. More specifically, the quantities involved in the estimator are the work exponential averages related to the forward and backward directions of the process and the free energy difference between the end states. Such free energy difference can be estimated without resorting to additional methodologies or data, but exploiting the available work measurements in the Bennett acceptance ratio method. Despite the fact that work exponential averages give strongly biased free energy profiles, a simple combination of them, supplied with an accurate estimate of the free energy difference between the end states, provides good free energies, even for fast pulling velocities of the control parameter. Numerical tests have been performed on a deterministic non-Hamiltonian dynamic system (the folding/unfolding process of one alanine deca-peptide) and on a stochastic toy model (a particle which moves into a one-dimensional potential according to Langevin dynamics). In these tests we compare our potential of mean force estimator to the unidirectional Jarzynski equality and to other bidirectional estimators that have appeared in the literature recently.

I. Introduction

The nonequilibrium work theorem by Jarzynski,¹

$$\langle e^{-\beta W} \rangle = e^{-\beta \Delta F}, \quad (1.1)$$

relates the work performed on a system during a nonequilibrium process, to the free energy difference ΔF between two equilibrium states of that system. The angular brackets denote an average over all possible realizations of the process, during which the system evolves in time as a control parameter is varied from an initial to a final value. W is the external work performed on the system during one realization and β is the inverse temperature of a heat reservoir with which the system is equilibrated prior to the start of each realization of the process. Several derivations of eqn (1.1),^{1–12} as well as experimental tests,^{13,14} have been provided. Eqn (1.1) may be viewed as a straightforward consequence of a more general work theorem originally derived by Crooks for microscopically reversible Markovian systems in the context of Monte Carlo simulations.^{3,15} The Crooks nonequilibrium work theorem relates the probability of a trajectory to the probability of its time reversal:

$$\frac{p(A \rightarrow B)}{p(A \leftarrow B)} = \exp[\beta(W_{A \rightarrow B} - \Delta F)], \quad (1.2)$$

where $p(A \rightarrow B)$ is the joint probability of taking the microstate A from a canonical distribution with Hamiltonian H_A

and of performing the transformation to the microstate B with Hamiltonian H_B . $p(A \leftarrow B)$ is the analogous joint probability for the time reversed trajectory. In eqn (1.2), $W_{A \rightarrow B}$ is the work performed on the system during the trajectory $A \rightarrow B$ and $\Delta F = F_B - F_A$. Since its original formulation, eqn (1.2), as well as the Jarzynski nonequilibrium work theorem, has been the object of intense research.^{8,15–24} Recently, Shirts *et al.* have demonstrated²⁵ that eqn (1.2) can be exploited in the context of maximum likelihood methods to derive the so-called Bennett acceptance ratio,²⁶ which is the best asymptotically unbiased method for determining the free energy difference between two states given work measurements collected from nonequilibrium processes switching the system between such states. In the same article,²⁵ the authors have also proved that it is possible to interpret eqn (1.1) as the maximum likelihood estimator for the free energy difference within the limit that samples are drawn from only one distribution.

While theoretically remarkable, eqn (1.1) is known to furnish strongly biased free energy estimates,^{9,27–29} mainly because the exponential average depends crucially on a small fraction of realizations that transiently violate the second law of thermodynamics (*i.e.*, realizations that yield a negative dissipated work). Since such realizations are very unlikely to occur among a collection of fast rate realizations, it is clear that the potential of mean force^{30,31} (PMF) cannot be determined accurately by the direct application of eqn (1.1). In this respect Hummer made several tests aimed at the calculation of the PMF between two methane molecules in water,²⁸ concluding that the direct exponential average is likely to suffer from large systematic statistical uncertainties that can be alleviated using cumulant estimates of the free energy. The same conclusion was put forward by Park and Schulten²⁷ and by

^a Dipartimento di Chimica, Università di Firenze,
Via della Lastruccia 3, I-50019 Sesto Fiorentino, Italy

^b European Laboratory for Non-linear Spectroscopy (LENS),
Via Nello Carrara 1, I-50019 Sesto Fiorentino, Italy.
E-mail: chelli@chim.unifi.it

Oberhofer *et al.*⁹ Means of improving the computational efficiency of the Jarzynski nonequilibrium work theorem include, besides the cumulant expansion approach,²⁸ biased path sampling^{7,32,33} and use of large time steps.^{34,35}

With regard to the Crooks nonequilibrium work theorem, Shirts and Pande recently showed²⁹ that the Bennett acceptance ratio, which is indeed based²⁵ on the Crooks theorem, can be significantly more accurate than eqn (1.1) for recovering free energy differences, and even more efficient than thermodynamic integration.³⁰ The main limitation of the method lies in the fact that it is not directly applicable to the calculation of the PMF along a given collective coordinate, but rather to free energy differences between end states. In principle, the Bennett acceptance ratio could be used to recover PMF profiles, but only at a very high computational cost. In fact, as Hummer pointed out,²⁸ several equilibrium simulations should be performed at closely spaced sampled points along the collective coordinate. It also appears clear that such a protocol is hardly usable in pulling nonequilibrium experiments.^{13,16}

Inspired by maximum likelihood arguments²⁵ and by the concept of path-ensemble average in systems driven far from equilibrium,¹⁵ we have recently presented a methodology to estimate the PMF along a given collective coordinate.³⁶ The basic advantage of the method with respect to the Jarzynski nonequilibrium work theorem is that it furnishes the PMF with greater accuracy, comparable to that of the Bennett acceptance ratio from which it is basically derived. However, unlike the Bennett method, which is devised for determining only free energy differences between end states, our approach provides the full PMF. A very similar PMF estimator has been also proposed by Feng and Crooks as an intermediate step to calculate the thermodynamic length of a system.³⁷ In a very recent article, Minh and Adib,³⁸ taking advantage of similar arguments,¹⁵ have developed a PMF estimator which reduces to the Bennett acceptance ratio^{25,26} at the end states. From numerical tests performed on a Brownian toy model, the authors found that their PMF estimator outperforms that of ref. 36, especially in the intermediate states along the collective coordinate. These recent bidirectional methods aimed at calculating the PMF all succeed in bypassing the intrinsic problem of the bias in the work exponential averages by means of more or less complicate expressions based on maximum likelihood arguments (the case of refs. 36 and 37) or on the optimal combination of the path distributions from the forward and backward directions of a process (the case of ref. 38).

In this article we present a very simple PMF estimator, which uses measurements of the work performed on a system during nonequilibrium pulling experiments in the forward and backward directions of a process. In particular, the estimator is based on a linear combination of forward and backward Jarzynski-like work exponential averages and on an estimate of the free energy difference between the end states. Such free energy difference is determined by exploiting the work measurements in the Bennett acceptance ratio method. The use of work exponential averages is indeed a remarkable fact considering that the accuracy of our bidirectional estimator, contrarily to the single work exponential averages, is only

slightly affected by the velocity of the nonequilibrium realizations. This will be shown here through a comparative analysis involving the proposed estimator (eqn (2.7) of the present work), those of refs. 36 and 38, and the Jarzynski equality.¹ The PMF will be calculated for two exemplary but not trivial cases: the folding/unfolding process of one alanine decapeptide in the context of steered molecular dynamics simulations and the externally driven motion of a Brownian particle along a one-dimensional potential.

In the next section we present some theoretical considerations along with the PMF estimator. We then describe the studied systems and several technical aspects in section III. The results are given in section IV, while conclusive remarks are discussed in section V.

II. Theoretical background

The PMF³⁰ of a system with N particles is strictly the potential that gives the mean force, estimated over all the configurations of $n + 1, \dots, N$ particles, acting on a particle j (with $j = 1, 2, \dots, n$) by keeping the particles $1, \dots, n$ fixed.³¹ In a more practical way, the PMF can be used to know how the free energy changes as a function of a collective coordinate of the system. Such a collective coordinate, ζ , is a general function $\zeta'(\mathbf{q})$ of the Cartesian coordinates of the system particles. The PMF, $\Phi(\zeta)$, is defined from the distribution function of ζ as

$$\Phi(\zeta) = \Phi(\zeta^*) - \beta^{-1} \ln(\int \delta(\zeta'(\mathbf{q}) - \zeta) e^{-\beta V(\mathbf{q})} d\mathbf{q}), \quad (2.3)$$

where $\Phi(\zeta^*)$ is an arbitrary constant, $\delta(\zeta'(\mathbf{q}) - \zeta)$ is the Dirac δ function for the coordinate ζ and $V(\mathbf{q})$ is the potential energy of the system.

Using nonequilibrium pulling techniques, such as optical tweezers¹⁶ or steered molecular dynamics simulations,²⁷ it is possible to estimate the PMF as a function of the value of a control parameter λ used to drive the system along the chosen ζ coordinate.^{1,36,38} Strictly speaking, this kind of PMF does not refer to the real system, but rather to a fictitious system whose potential energy is

$$V'(\mathbf{q}; \lambda) = V(\mathbf{q}) + \frac{k}{2} [\zeta'(\mathbf{q}) - \lambda]^2, \quad (2.4)$$

where the additional (harmonic) potential³⁹ is used to produce the nonequilibrium realizations through the externally driven control parameter λ . Using known nonequilibrium work relations,^{1,36,38} one may estimate the λ -dependent PMF, which is defined as

$$\Phi(\lambda) = \Phi(\lambda^*) - \beta^{-1} \ln(\int e^{-\beta V'(\mathbf{q}; \lambda)} d\mathbf{q}), \quad (2.5)$$

where $\Phi(\lambda^*)$ is the usual arbitrary constant. As a matter of fact, it has been shown²⁷ that eqns (2.3) and (2.5) are equivalent if the stiff spring approximation holds. However, reweighting methods have been devised to recover the real PMF (eqn (2.3)) from nonequilibrium work measurements^{5,38} that use external driving potentials such as that of eqn (2.4). In the present work we will treat the λ -dependent PMF (eqn (2.5)), leaving the formulation of reweighting approaches to further investigations. We point out, however, that the method proposed here is already usable in numerical experiments because the stiff spring approximation can be enforced

easily with an appropriate choice of the harmonic force constant in eqn (2.4).

We start by noting that, if the work performed on a system is known for two collections of nonequilibrium realizations during which the control parameter λ (bound to a collective coordinate ζ) is switched from the value λ_a to the value λ_b (forward, or F , realizations) and vice versa (backward, or B , realizations), then two independent PMF estimates based on the Jarzynski equality can be written as

$$\begin{aligned}\Phi_F(\lambda) &= -\beta^{-1} \ln \langle e^{-\beta W_F(\lambda)} \rangle, \\ \Phi_B(\lambda) &= -\beta^{-1} \ln \langle e^{-\beta W_B(\lambda)} \rangle,\end{aligned}\quad (2.6)$$

where $W_F(\lambda)$ is the work done on the system to switch the control parameter from λ_a to λ during the F realizations and $W_B(\lambda)$ is the work done on the system to switch the control parameter from λ_b to λ during the B realizations. Clearly, λ may take any value between λ_a and λ_b . We stress that, since the initial microstates of the F and B realizations belong to different thermodynamic states, it is not possible to combine $\Phi_F(\lambda)$ and $\Phi_B(\lambda)$ directly to obtain an improved PMF estimator. The only possible combination calls into play $\Phi_F(\lambda_b)$ and $\Phi_B(\lambda_a)$ to eventually get the free energy difference $\Delta F_{ab} = F(\lambda_b) - F(\lambda_a)$ between the end states.²⁹ However, the provision of a reliable estimate of ΔF_{ab} , or even the simple knowledge of it from experimental data, would allow one to use $\Phi_B(\lambda)$ to get an additional estimate of $\Phi_F(\lambda)$, say $\Phi'_F(\lambda)$, through the simple relationship $\Phi'_F(\lambda) = \Delta F_{ab} + \Phi_B(\lambda)$. Analogously, the relationship $\Phi'_B(\lambda) = -\Delta F_{ab} + \Phi_F(\lambda)$ allows us to get an estimate of $\Phi_B(\lambda)$ from the knowledge of $\Phi_F(\lambda)$. Taking advantage of this, we propose the following simple estimate of the PMF

$$\begin{aligned}\Phi(\lambda) &= -\beta^{-1} \ln [e^{-\beta \Phi_F(\lambda)} + e^{-\beta \Phi'_F(\lambda)}] + c \\ &= -\beta^{-1} \ln [\langle e^{-\beta W_F(\lambda)} \rangle + e^{-\beta \Delta F_{ab}} \langle e^{-\beta W_B(\lambda)} \rangle] + c,\end{aligned}\quad (2.7)$$

where c is an arbitrary constant. Of course, an equivalent estimator can be written using $\Phi_B(\lambda)$ and $\Phi'_B(\lambda)$. Basically, to employ eqn (2.7), one needs to supply a strategy for determining ΔF_{ab} , resorting, if possible, to the data already available, *i.e.*, the nonequilibrium work measurements in the F and B directions. In this respect a candidate approach could be to combine $\Phi_F(\lambda_b)$ and $\Phi_B(\lambda_a)$ (from eqn (2.6)) as suggested by Shirts and Pande in ref. 29. However, as the authors themselves showed,²⁹ the Bennett acceptance ratio method²⁶ is significantly more efficient than work exponential averages in recovering free energy differences. Accordingly, we chose the Bennett method to evaluate ΔF_{ab} . In this respect we notice that other bidirectional PMF estimators (eqn (16) of ref. 36 and eqns (7) and (10) of ref. 38) also use the quantity ΔF_{ab} estimated from the Bennett method to calculate the whole free energy profile.

III. Numerical tests: methods and systems

As stated above, to assess the performances of eqn (2.7) in relation to the well known unidirectional Jarzynski method (eqn (1.1)) and other bidirectional methods, we have performed PMF estimates related to the unfolding/refolding process of one alanine deca-peptide (A_{10}) at finite temperature

and to the externally driven motion of a Brownian particle experiencing a one-dimensional potential.

A Alanine deca-peptide

In the case of A_{10} , the employed work measurements have been taken from earlier computer experiments whose technical details are given elsewhere.²¹ However, for the sake of completeness, in this section we give again a description of the system and some technical details on the simulations.

Pulling numerical experiments have been performed using constant-volume constant-temperature steered molecular dynamics simulations, taking the end-to-end distance of A_{10} as collective coordinate ζ . In particular, ζ is the distance between the nitrogen atom of the N-terminus amino-acid (constrained to a fixed position) and the nitrogen atom of the C-terminus amino-acid (constrained to move along a fixed direction). In agreement with earlier studies,²⁷ the values of the control parameter λ in the folded and unfolded states of A_{10} are taken to be 15.5 and 31.5 Å, respectively. The unfolding process of A_{10} has been arbitrarily chosen to be the forward, F , direction. In the context of our notation, we therefore set $\lambda_a = 15.5$ Å and $\lambda_b = 31.5$ Å. It should be noted that in general the end-to-end distance does not uniquely determine the configurational state of polypeptides. However, in the specific case of A_{10} , the equilibrium distribution at $\lambda = \lambda_a$ corresponds to an ensemble of microstates tightly peaked around the α -helix form, as for this end-to-end distance alternative structures are virtually impossible. The same holds true for the state corresponding to $\lambda = \lambda_b$, which basically represents an almost fully elongated configuration of the peptide. This implies that these two thermodynamic states can be effectively sampled using relatively few microstates obtained from equilibrium molecular dynamics simulations at the given λ values. The initial microstates for the F and B realizations have therefore been randomly picked (every 5 ps) from two standard molecular dynamics simulations where the usual system Hamiltonian is supplied with an additional harmonic potential, $k/2(\zeta - \lambda)^2$, with λ fixed to λ_a and λ_b , respectively. The force constant k is taken to be 800 kcal mol⁻¹ Å⁻², corresponding in this system to a very stiff spring regime. In both equilibrium molecular dynamics simulations and in the subsequent series of steered molecular dynamics simulations, constant temperature (300 K) has been enforced using a Nosé-Hoover thermostat.^{40,41} The force field has been taken from ref. 42. Given the limited size of the sample, no cutoff radius has been imposed on the atomic pair interactions and no periodic boundary conditions have been applied. The equations of motion have been integrated through a multiple time step technique as implemented in the ORAC program.⁴³ For each type of process, F and B , we generated 10⁴ realizations guiding λ from λ_a to λ_b (F realizations) or from λ_b to λ_a (B realizations) with the harmonic potential reported above. The time-dependence of λ determines the pulling velocity of the realizations and in general their time schedule. In our case, λ varies linearly with the time, *i.e.* $\lambda = \lambda_a + \dot{\lambda}t$ for the F realizations and $\lambda = \lambda_b - \dot{\lambda}t$ for the B ones. Therefore, the duration time of each pulling realization is $(\lambda_b - \lambda_a)/\dot{\lambda}$. The value of the work function at a

given time t during a realization is calculated by integrating the partial derivative of the harmonic potential with respect to time from time zero to time t . Six series of B/F work measurements differing only in the pulling velocity have been performed ($\dot{\lambda} = 80, 160, 320, 533, 800$ and 1600 \AA ns^{-1}).

B Brownian particle

The case of a one-dimensional particle moving according to overdamped Langevin dynamics is inspired by ref. 44, in the same fashion as ref. 38. In particular, we have carried out steered Langevin simulations of one particle obeying the time-dependent potential energy $V'(x; \lambda) = V(x) + k/2[\zeta'(x) - \lambda]^2$, where the collective coordinate $\zeta'(x)$ simply corresponds to the particle position (*i.e.* $\zeta'(x) = x$) and $V(x)$ is the real one-dimensional potential energy. The time-dependent harmonic potential is used to produce the nonequilibrium realizations through the externally driven control parameter. As for A_{10} , λ is chosen to vary linearly with the time from $\lambda_a = -1.5$ to $\lambda_b = 1.5$ (F realizations) and vice versa (B realizations). The diffusion coefficient and the inverse temperature β are both 1, and we use a time step of 0.001. The force constant k is 15. The work performed on the system was accumulated according to Hummer.⁴⁴ The potential energy of the system is

$$V(x) = 5(x^2 - 1)^2 + fx, \quad (3.8)$$

where f is a parameter (kept fixed during the simulations) used to modulate the shape of $V(x)$. In these tests, we have analyzed three types of potential energy: $f = 0, 3, 9$. It is known that the free energy profile of the unperturbed system corresponds to $V(x)$.⁴⁴ However, as stated above, in the present context we are interested in the λ -dependent PMF. Given the extreme simplicity of the potential energy $V(x)$, the exact λ -dependent PMF to be used as a reference can be calculated directly from eqn (2.5) through numerical integration. Three series of B/F work measurements, with different pulling velocities, have been performed for each value of f : $\dot{\lambda} = 4 \times 10^{-3}, 3 \times 10^{-2}$, and $6 \times 10^{-2} \text{ step}^{-1}$ (corresponding to 750, 100, and 50 simulation steps, respectively). For each series, we have generated $10^4 F$ and $10^4 B$ realizations. The initial particle positions for the F and B realizations have been taken from equilibrium simulations at fixed λ .⁴⁵ Each realization has been performed with a different seed for random number generation.

IV. Numerical tests: results

A Alanine deca-peptide

From now on we denote the various estimates of the PMF with $\Phi_x(\lambda)$, where the subscript indicates the kind of estimator:⁴⁶ $x \equiv \text{JF, JB}$ for the Jarzynski equalities in the F and B directions; $x \equiv \text{CP, MA, CMP}$ for the bidirectional estimators related to eqn (2.7) of the present work, eqn (7) of ref. 38, and eqn (16) of ref. 36, respectively. Clearly, for the bidirectional estimators, the total number n of employed work measurements corresponds to the sum $n_F + n_B$, n_F and n_B being the number of F and B realizations taken into account. In the present calculations we consider only the case $n = 2n_B = 2n_F$, though the bidirectional methods can be applied with arbitrary

n_B and n_F . In this respect we point out that the most efficient value of the ratio n_F/n_B in applying the Bennett acceptance ratio method, namely to estimate ΔF_{ab} , has been shown to be always close to one.²⁶ The limits $n_F \gg n_B$ and $n_F \ll n_B$ are significantly less efficient sometimes by three or four orders of magnitude.

The “exact” PMF that we use as reference is denoted with $\Phi_{\text{TI}}(\lambda)$ and has been calculated through thermodynamic integration³⁰ on the system A_{10} plus a harmonic potential used to constrain the collective coordinate around the equilibrium value (the force constant is equal to that used in steered molecular dynamics simulations). Of course, the various PMF estimators may differ from $\Phi_{\text{TI}}(\lambda)$ for an arbitrary constant, say q . Therefore, in order to make consistent comparisons, we have determined q using a least-squares procedure. Specifically, the constant q to be added to $\Phi_x(\lambda)$ is calculated by solving the equation $\partial \eta^2 / \partial q = 0$, where

$$\eta^2 = \frac{1}{N} \sum_{i=1}^N [q + \Phi_x(\lambda_i) - \Phi_{\text{TI}}(\lambda_i)]^2. \quad (4.9)$$

The resolution for λ has been arbitrarily chosen to be 0.2 \AA , so that $N = 81$ in eqn (4.9). The values of η obtained from the PMF estimates $\Phi_x(\lambda)$ ($x \equiv \text{JF, JB, CP, MA, CMP}$) for different pulling velocities and for different numbers n of employed realizations are reported in Table 1. The η values reported in

Table 1 A_{10} case: η values (in kJ mol^{-1}) calculated using $\Phi_{\text{CP}}(\lambda)$ (eqn (2.7)), $\Phi_{\text{JF}}(\lambda)$ (eqn (1.1)), $\Phi_{\text{JB}}(\lambda)$ (eqn (1.1)), $\Phi_{\text{CMP}}(\lambda)$ (eqn (16) of ref. 36), and $\Phi_{\text{MA}}(\lambda)$ (eqn (7) of ref. 38) for various pulling velocities $\dot{\lambda}$ (in \AA ns^{-1}) and for $n = 2 \times 10^4, 10^4, 10^3, 10^2$ (sets A, B, C, and D, respectively). The standard deviation of η is reported in parentheses as the error on the last digit. Because of the low number of independent sets, the standard deviation is meaningless for the sets A and B. For the set C, the standard deviation is calculated over 20 and 10 estimates of η (bidirectional and unidirectional methods, respectively). For the set D, the standard deviation is calculated over 200 and 100 estimates of η (bidirectional and unidirectional methods, respectively)

	$\dot{\lambda}$	$\Phi_{\text{CP}}(\lambda)$	$\Phi_{\text{JF}}(\lambda)$	$\Phi_{\text{JB}}(\lambda)$	$\Phi_{\text{CMP}}(\lambda)$	$\Phi_{\text{MA}}(\lambda)$
A	80	0.5			0.5	0.2
	160	0.8			1.4	0.7
	320	0.5			1.4	0.7
	533	1.0			3.2	1.0
	800	4.1			2.9	4.1
	1600	6.7			9.6	6.7
B	80	0.5	1.9	0.8	0.5	0.2
	160	0.8	2.5	3.1	1.3	0.7
	320	0.9	4.9	3.9	1.5	1.0
	533	1.1	8.9	7.9	3.4	1.2
	800	4.2	11.8	13.8	4.3	4.2
	1600	6.8	18.8	30.1	9.5	6.8
C	80	0.6(4)	2.0(4)	1.1(3)	0.8(3)	0.5(2)
	160	0.9(5)	3(1)	3(1)	1.4(4)	0.9(5)
	320	2.1(9)	7(2)	6(2)	2.5(7)	2.0(9)
	533	4(1)	10(2)	11(3)	4(2)	4(1)
	800	6(2)	13(2)	19(5)	7(2)	6(2)
	1600	7(1)	21(2)	30(1)	9(1)	7(1)
D	80	1.1(6)	2.7(9)	2(1)	1.2(4)	1.0(5)
	160	2(1)	5(1)	5(2)	2.2(9)	2(1)
	320	4(2)	8(2)	11(4)	4(1)	4(2)
	533	6(3)	12(2)	18(5)	7(2)	6(3)
	800	8(2)	16(2)	26(5)	8(2)	8(2)
	1600	8(2)	24(3)	31(1)	8(2)	8(2)

the Table correspond to the average of several estimates recovered from non-overlapping sets of work measurements. For example, the results related to the bidirectional PMF estimators $\Phi_{\text{CP}}(\lambda)$, $\Phi_{\text{MA}}(\lambda)$, and $\Phi_{\text{CMP}}(\lambda)$ for $n = 100$ ($n_F = n_B = 50$) have been averaged over 200 sets of independent data, such that $200 \times n$ equals 2×10^4 (*i.e.*, the total number of F and B work measurements). In the case of $\Phi_{\text{JF}}(\lambda)$ and $\Phi_{\text{JB}}(\lambda)$, with $n = 100$, the number of independent sets considered for averaging is instead 100, because the number of available work measurements for each direction of the process is 10^4 . This implies that Jarzynski PMF estimates cannot be produced with $n = 2 \times 10^4$. In Table 1 we also report the standard deviation of η calculated over the values recovered from the independent sets of measurements.

The general worsening of the accuracy of the PMF estimators with increasing pulling velocity and with decreasing number of realizations n is expected on the basis of statistical reasons. The remarkable result is that the performances of both Jarzynski equalities in the F and B directions are much worse than those of the other PMF estimators, especially when the pulling velocity is increased. In fact, at high pulling velocities, the differences of η between the unidirectional and bidirectional methods exceed the standard deviations significantly. In this respect, it should be noted that for $\Phi_{\text{JF}}(\lambda)$ and $\Phi_{\text{JB}}(\lambda)$ the η quantity actually gives an underestimate of the error. In fact, if on the one hand Jarzynski PMF estimators are accurate at the beginning of the reaction path, *i.e.* where the dissipated work is small, on the other hand their performances become worse at the end of the reaction path due to bias arising from dissipation. This nonuniform distribution of the error through the reaction path suggests that the actual error cannot simply be determined by considering the overall PMF curve as implied by eqn (4.9). Despite this, it is evident that an analysis made on the basis of η does not prevent one from drawing conclusions about the relative performances of the PMF estimators under consideration.

Furthermore, it is worth noting that, according to Minh and Adib's findings,³⁸ $\Phi_{\text{CMP}}(\lambda)$ is the least well performing among the bidirectional PMF estimators. Notwithstanding, the differences in the η quantity do not exceed few kJ mol^{-1} , often being smaller than the standard deviations of the estimates. Comparing $\Phi_{\text{CP}}(\lambda)$ with $\Phi_{\text{MA}}(\lambda)$, we note that, for high pulling velocities, they are numerically equivalent, while

the latter estimator seems to work slightly better for slow processes. However, the differences always being of the order of few kJ mol^{-1} (*e.g.*, for set C of Table 1 these differences are below the standard deviation of η), we cannot draw any certain and general conclusions regarding the relative accuracy of the two estimators $\Phi_{\text{CP}}(\lambda)$ and $\Phi_{\text{MA}}(\lambda)$. As far as the A_{10} system is concerned, they indeed appear equivalently good estimators. As a matter of fact, we will see in section IVB that, for the Brownian particle case, $\Phi_{\text{CP}}(\lambda)$ works slightly better than $\Phi_{\text{MA}}(\lambda)$ for slow pulling velocities of the process.

A visual comparison between $\Phi_{\text{JF}}(\lambda)$, $\Phi_{\text{JB}}(\lambda)$, and $\Phi_{\text{CP}}(\lambda)$ with $n = 10^4$ is given in Fig. 1 for three representative pulling velocities ($\Phi_{\text{TI}}(\lambda)$ is also reported as reference). The much better performance of $\Phi_{\text{CP}}(\lambda)$ with respect to both unidirectional Jarzynski equalities is evident. We point out that the discrepancies between $\Phi_{\text{TI}}(\lambda)$ and $\Phi_{\text{CP}}(\lambda)$ are significant only at very high pulling velocity (800 \AA ns^{-1}). Such velocity means that one tries to irreversibly unfold or refold the A_{10} peptide in less than 20 ps, which is indeed a very dissipative regime. The greater the work dissipated, the less accurate $\Phi_{\text{JF}}(\lambda)$ and $\Phi_{\text{JB}}(\lambda)$ become. Nonetheless the degradation in performance of their combined form (in the form of eqn (2.7)) with increasing pulling velocity is much less dramatic than that of the unidirectional Jarzynski equalities. We also remark that this fact must not be ascribed to statistical reasons related to the number of realizations, because the total number of realizations employed in the estimators is the same.

B Brownian particle

The results obtained from the steered dynamics of a Brownian particle are summarized in Tables 2–4, where we report the values of η and the related standard deviations for the three systems with unperturbed Hamiltonians corresponding to $f = 0, 3, 9$ (see eqn (3.8)). The performances have been analyzed for different pulling velocities and different numbers n of realizations. In this case, η has been computed (see eqn (4.9)) in the interval $-1.5 \leq \lambda \leq 1.5$ with a λ -resolution of 0.06, for a total of $N = 51$ points along the domain of λ . As usual, η corresponds to the average of several estimates calculated from non-overlapping sets of work measurements (see section IV A for a detailed explanation). Overall, the data are consistent with those obtained for the A_{10}

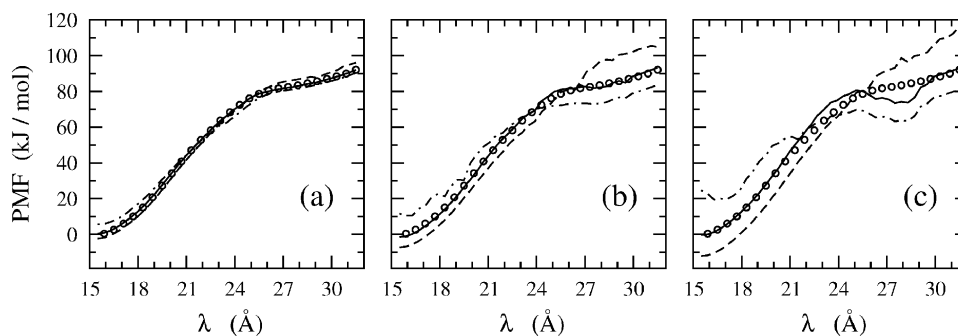


Fig. 1 Comparison between $\Phi_{\text{CP}}(\lambda)$ (solid line), $\Phi_{\text{JF}}(\lambda)$ (dashed line), and $\Phi_{\text{JB}}(\lambda)$ (dot-dashed line) for the A_{10} peptide (with $n = 10^4$) at various pulling velocities $\dot{\lambda}$ (from panel (a) to panel (c): $\dot{\lambda} = 160, 533$, and 800 \AA ns^{-1}). The exact PMF, $\Phi_{\text{TI}}(\lambda)$, is also reported (circles). We have arbitrarily chosen $\Phi_{\text{TI}}(15.5) = 0$, while the additive constants for the $\Phi_{\text{CP}}(\lambda)$, $\Phi_{\text{JF}}(\lambda)$ and $\Phi_{\text{JB}}(\lambda)$ curves have been determined by minimizing the η quantity of eqn (4.9).

Table 2 Brownian particle case ($f = 0$): η values calculated using $\Phi_{CP}(\lambda)$ (eqn (2.7)), $\Phi_{JF}(\lambda)$ (eqn (1.1)), $\Phi_{JB}(\lambda)$ (eqn (1.1)), $\Phi_{CMP}(\lambda)$ (eqn (16) of ref. 36), and $\Phi_{MA}(\lambda)$ (eqn (7) of ref. 38) for various pulling velocities λ (in 10^{-3} step $^{-1}$) and for $n = 2 \times 10^4, 2 \times 10^3, 10^2$ (sets A, B, and C, respectively). The standard deviation of η is reported in parentheses as the error on the last digit. Because of the low number of independent sets, the standard deviation is meaningless for the set A. For the set B, the standard deviation is calculated over 10 and 5 estimates of η (bidirectional and unidirectional methods, respectively). For the set C, the standard deviation is calculated over 200 and 100 estimates of η (bidirectional and unidirectional methods, respectively)

	λ	$\Phi_{CP}(\lambda)$	$\Phi_{JF}(\lambda)$	$\Phi_{JB}(\lambda)$	$\Phi_{CMP}(\lambda)$	$\Phi_{MA}(\lambda)$
A	4	0.02			0.44	0.03
	30	0.86			3.03	0.86
	60	1.03			3.90	1.03
B	4	0.13(3)	1.8(1)	1.7(2)	0.47(7)	0.13(3)
	30	0.7(4)	6.7(5)	8.1(3)	3.2(3)	0.7(4)
	60	0.8(4)	8.8(4)	9.9(1)	4.0(2)	0.8(4)
C	4	0.4(3)	2.1(5)	2.0(6)	0.7(2)	0.4(3)
	30	0.9(5)	8(1)	8.6(7)	3.6(3)	0.9(5)
	60	0.9(4)	10(1)	10.3(6)	4.4(2)	0.9(4)

Table 3 η values and standard deviations for the Brownian particle case $f = 3$. See Table 2 for details

	λ	$\Phi_{CP}(\lambda)$	$\Phi_{JF}(\lambda)$	$\Phi_{JB}(\lambda)$	$\Phi_{CMP}(\lambda)$	$\Phi_{MA}(\lambda)$
A	4	0.02			0.41	0.03
	30	1.33			3.28	1.33
	60	2.19			4.17	2.19
B	4	0.08(3)	1.79(9)	1.57(7)	0.44(5)	0.08(3)
	30	1.3(4)	6.1(5)	8.8(3)	3.3(3)	1.3(4)
	60	1.9(5)	7.6(4)	11.0(1)	4.24(9)	1.9(5)
C	4	0.4(3)	2.0(4)	1.9(6)	0.7(2)	0.4(3)
	30	1.2(7)	7.4(9)	9.5(8)	3.7(4)	1.2(7)
	60	1.6(7)	8.8(9)	11.6(7)	4.5(3)	1.6(7)

Table 4 η values and standard deviations for the Brownian particle case $f = 9$. See Table 2 for details

	λ	$\Phi_{CP}(\lambda)$	$\Phi_{JF}(\lambda)$	$\Phi_{JB}(\lambda)$	$\Phi_{CMP}(\lambda)$	$\Phi_{MA}(\lambda)$
A	4	0.02			0.40	0.04
	30	2.19			3.64	2.19
	60	4.04			4.89	4.04
B	4	0.08(5)	1.5(1)	1.6(1)	0.41(5)	0.09(5)
	30	2.1(4)	4.2(3)	9.1(1)	3.7(3)	2.1(4)
	60	4.0(4)	5.0(3)	12.2(2)	4.9(2)	4.0(4)
C	4	0.4(2)	1.7(4)	1.8(4)	0.6(2)	0.4(2)
	30	2.5(8)	4.9(6)	10(1)	4.1(6)	2.5(8)
	60	4.1(8)	5.8(7)	13.1(9)	5.3(5)	4.1(8)

system. In fact, we note that $\Phi_{CP}(\lambda)$ and $\Phi_{MA}(\lambda)$ agree with the analytical PMF (eqn (2.5)) better than $\Phi_{CMP}(\lambda)$ does (as indeed Minh and Adib observed³⁸), and that all bidirectional PMF estimators strongly outperform the Jarzynski equality in both F and B directions. As observed for A_{10} , numerical equivalence between $\Phi_{CP}(\lambda)$ and $\Phi_{MA}(\lambda)$ occurs for high pulling velocities. However, at variance with the A_{10} system, at the slowest pulling velocity $\Phi_{CP}(\lambda)$ works slightly better than $\Phi_{MA}(\lambda)$. Again, we point out that such features, though quite systematic in this system, do not allow one to draw final conclusions regarding the optimal PMF estimator, which rather seems to be system dependent.

The PMFs $\Phi_{JF}(\lambda)$, $\Phi_{JB}(\lambda)$, and $\Phi_{CP}(\lambda)$ for the three Brownian systems, with $n = 2 \times 10^3$ and pulling velocity of 4×10^{-3} step $^{-1}$ are reported in Fig. 2 (the exact PMF from eqn (2.5) is also reported as a reference). Also in this case, the better performance of $\Phi_{CP}(\lambda)$ with respect to both unidirectional Jarzynski approaches is evident. Note that the differences between $\Phi_{CP}(\lambda)$ and the exact PMF for $f = 0$ are emphasized by the y -scale of the figure and are only due to numerical error.

The fact that eqn (2.7) works fine for slow pulling velocities should not come as a surprise. Indeed, this estimator corresponds to the sum of two asymptotically exact estimators, namely the forward and backward Jarzynski-like work exponential averages (eqn (1.1)). Of course, this implies that eqn (2.7) is asymptotically exact too. Instead, what one may find surprising and encouraging is that, even for high pulling velocity, eqn (2.7) still continues to be a good PMF estimator. In such a case the reliability of eqn (2.7) lies in the fact that it represents the optimal way of combining F and B work measurements. This can be understood from the comparison of eqn (2.7) with Minh and Adib's PMF estimator (eqn (7) of ref. 38) in the limit of highly dissipative realizations. For the sake of convenience, we report here the Minh and Adib's estimator:

$$\Phi(\lambda) = -\beta^{-1} \ln \left[\left\langle \frac{n_F e^{-\beta W_F(\lambda)}}{n_F + n_B e^{\beta[-W_F(\lambda_b) + \Delta F_{ab}]}} \right\rangle_F + \left\langle \frac{n_B e^{\beta[W_B(\lambda_a) - W_B(\lambda)]}}{n_F + n_B e^{\beta[W_B(\lambda_a) + \Delta F_{ab}]}} \right\rangle_B \right], \quad (4.10)$$

where we have used the notation introduced for eqns (2.6) and (2.7). For high pulling velocity, the first average can be

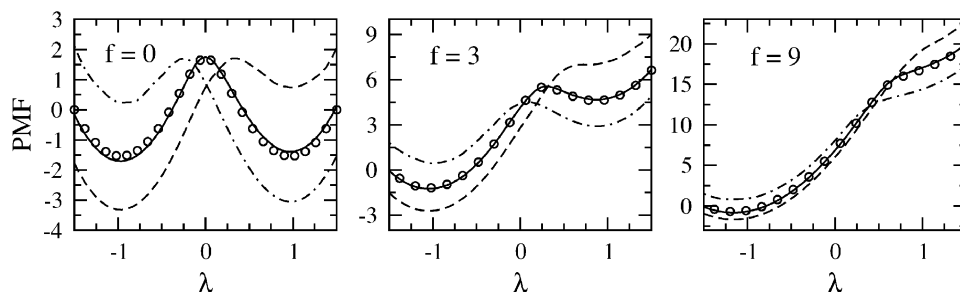


Fig. 2 Comparison between $\Phi_{CP}(\lambda)$ (solid line), $\Phi_{JF}(\lambda)$ (dashed line), and $\Phi_{JB}(\lambda)$ (dot-dashed line) for the Brownian systems corresponding to $f = 0, 3, 9$, with $n = 2 \times 10^3$ and pulling velocity of 4×10^{-3} step $^{-1}$. The exact PMF $\Phi(\lambda)$ (eqn (2.5)) is also reported (circles). We have arbitrarily chosen $\Phi(-1.5) = 0$, while the additive constants for the $\Phi_{CP}(\lambda)$, $\Phi_{JF}(\lambda)$ and $\Phi_{JB}(\lambda)$ curves have been determined by minimizing the η quantity of eqn (4.9).

approximated to a simple work exponential average because, due to large dissipation, $W_F(\lambda_b) \gg \Delta F_{ab}$ so that in the denominator one can neglect $n_B \exp[\beta(-W_F(\lambda_b) + \Delta F_{ab})]$ with respect to n_F . Analogously, as the average over the B realizations is concerned, considering the same conditions of large dissipation (*i.e.* for the limit case $W_B(\lambda_a) \gg -\Delta F_{ab}$), one can neglect n_F with respect to $n_B \exp[\beta(W_B(\lambda_a) + \Delta F_{ab})]$. The ensuing expression of $\langle \cdots \rangle_B$ in eqn (4.10) corresponds exactly to the second work exponential average of eqn (2.7). The numerical equivalence between eqns (2.7) and (4.10) can be fully appreciated in the η values and their standard deviations reported in Tables 1–4.

V. Conclusions

In the context of systems driven far from equilibrium, we have presented an extremely simple bidirectional PMF estimator (eqn (2.7)) based on “Jarzynski-like” work exponential averages and on the free energy difference between end states estimated using the Bennett acceptance ratio method. Numerical tests have been done using steered molecular dynamics simulations of an alanine deca-peptide and steered Langevin dynamics of a one-dimensional particle. We have shown that our PMF estimator outperforms the Jarzynski equality significantly. The formal simplicity of eqn (2.7) and its excellent performance in recovering the exact PMF even for highly dissipative realizations can be understood noting that, in such situations, the algorithm recently proposed by Minh and Adib³⁸ practically reduces to eqn (2.7). This connection is fully evident from the numerical standpoint when performing pulling experiments at high velocity, *i.e.*, for large dissipative processes. We have however shown that this fact does not limit the use of eqn (2.7) to the case of fast pulling processes. Indeed, even when we are dealing with low dissipative processes, namely in those cases where the differences between the two algorithms should be more evident, Minh and Adib’s³⁸ estimator and eqn (2.7) still continue to show comparable performances.

In the framework of mechanical pulling experiments of systems driven out of equilibrium, the demonstrated accuracy of bidirectional PMF estimators,^{36,38} including eqn (2.7), for fast pulling velocities of the control parameter (*i.e.*, for computationally convenient simulations) is a very promising feature for making these techniques competitive with standard equilibrium non-Boltzmann methodologies also in more complex systems.

Acknowledgements

We thank Edward H. Feng (from University of California, Berkeley, California, USA) and Gavin E. Crooks (from Lawrence Berkeley National Laboratory, Berkeley, California, USA) for making available to us their still unpublished studies on “Far-from-equilibrium measurements of thermodynamic length”.³⁷ This work was supported by the European Union (Grant No. RII3-CT-2003-506350).

References

- 1 C. Jarzynski, *Phys. Rev. Lett.*, 1997, **78**, 2690.
- 2 C. Jarzynski, *Phys. Rev. E*, 1997, **56**, 5018.
- 3 G. E. Crooks, *J. Stat. Phys.*, 1998, **90**, 1481.
- 4 G. E. Crooks, *Phys. Rev. E*, 1999, **60**, 2721.
- 5 G. Hummer and A. Szabo, *Proc. Natl. Acad. Sci. U. S. A.*, 2001, **98**, 3658.
- 6 R. M. Neal, *Stat. Comput.*, 2001, **11**, 125.
- 7 S. X. Sun, *J. Chem. Phys.*, 2003, **118**, 5769.
- 8 D. J. Evans, *Mol. Phys.*, 2003, **101**, 1551.
- 9 H. Oberhofer, C. Dellago and P. L. Geissler, *J. Phys. Chem. B*, 2005, **109**, 6902.
- 10 M. A. Cuendet, *Phys. Rev. Lett.*, 2006, **96**, 120602.
- 11 M. A. Cuendet, *J. Chem. Phys.*, 2006, **125**, 144109.
- 12 R. D. Astumian, *Am. J. Phys.*, 2006, **74**, 683.
- 13 J. Liphardt, S. Dumont, S. B. Smith, I. Tinoco and C. Bustamante, *Science*, 2002, **296**, 1832.
- 14 F. Douarche, S. Ciliberto, A. Petrosyan and I. Rabbiosi, *Europhys. Lett.*, 2005, **70**, 593.
- 15 G. E. Crooks, *Phys. Rev. E*, 2000, **61**, 2361.
- 16 D. Collin, F. Ritort, C. Jarzynski, S. B. Smith, I. Tinoco and C. Bustamante, *Nature*, 2005, **437**, 231.
- 17 C. Jarzynski, *Phys. Rev. E*, 2006, **73**, 046105.
- 18 E. Schöll-Paschinger and C. Dellago, *J. Chem. Phys.*, 2006, **125**, 054105.
- 19 S. R. Williams, D. J. Searles and D. J. Evans, *Mol. Phys.*, 2007, **105**, 1059.
- 20 T. Ohkuma and T. Ohta, *J. Stat. Mech-Theory E*, 2007, P10010.
- 21 P. Procacci, S. Marsili, A. Barducci, G. F. Signorini and R. Chelli, *J. Chem. Phys.*, 2006, **125**, 164101.
- 22 R. Chelli, S. Marsili, A. Barducci and P. Procacci, *J. Chem. Phys.*, 2007, **126**, 044502.
- 23 R. Chelli, S. Marsili, A. Barducci and P. Procacci, *Phys. Rev. E*, 2007, **75**, 050101.
- 24 R. Chelli, S. Marsili, A. Barducci and P. Procacci, *J. Chem. Phys.*, 2007, **127**, 034110.
- 25 M. R. Shirts, E. Bair, G. Hooker and V. S. Pande, *Phys. Rev. Lett.*, 2003, **91**, 140601.
- 26 C. H. Bennett, *J. Comput. Phys.*, 1976, **22**, 245.
- 27 S. Park and K. Schulten, *J. Chem. Phys.*, 2004, **120**, 5946.
- 28 G. Hummer, *J. Chem. Phys.*, 2001, **114**, 7330.
- 29 M. R. Shirts and V. S. Pande, *J. Chem. Phys.*, 2005, **122**, 144107.
- 30 J. G. Kirkwood, *J. Chem. Phys.*, 1935, **3**, 300.
- 31 D. A. McQuarrie, *Statistical Mechanics*, Harper Collins Publishers, New York, USA, 1976.
- 32 F. M. Ytreberg and D. M. Zuckerman, *J. Chem. Phys.*, 2004, **120**, 10876.
- 33 F. M. Ytreberg and D. M. Zuckerman, *J. Chem. Phys.*, 2004, **121**, 5022.
- 34 W. Lechner, H. Oberhofer, C. Dellago and P. L. Geissler, *J. Chem. Phys.*, 2006, **124**, 044113.
- 35 H. Oberhofer, C. Dellago and S. Boresch, *Phys. Rev. E*, 2007, **75**, 061106.
- 36 R. Chelli, S. Marsili and P. Procacci, *Phys. Rev. E*, 2008, **77**, 031104.
- 37 E. H. Feng and G. E. Crooks, arXiv: 0807.0621, 2008.
- 38 D. D. L. Minh and A. B. Adib, *Phys. Rev. Lett.*, 2008, **100**, 180602.
- 39 The mathematical form of the additional potential is arbitrary. The only requirement is that it is able to constrain the collective coordinate $\zeta'(\mathbf{q})$ around a given λ value.
- 40 W. G. Hoover, *Phys. Rev. A*, 1985, **31**, 1695.
- 41 W. G. Hoover, *Phys. Rev. A*, 1986, **34**, 2499.
- 42 A. Mackerell, D. Bashford, M. Bellot, R. Dunbrack, J. Evanseck, M. Field, J. Gao, H. guo, S. Ha and D. Joseph-Mcarthy, *et al.*, *J. Phys. Chem. B*, 1998, **102**, 3586.
- 43 P. Procacci, T. A. Darden, E. Paci and M. Marchi, *J. Comput. Chem.*, 1997, **18**, 1848.
- 44 *Free Energy Calculations: Theory and Applications in Chemistry and Biology*, eds. C. Chipot and A. Pohorille, Springer, Berlin, 2007, vol. 86, p. 188.
- 45 $\lambda = \lambda_a$ for the F realizations and $\lambda = \lambda_b$ for the B realizations.
- 46 We will also use the same notation to indicate generically the corresponding PMF estimator.